Int. J. of GEOMATE, April, 2016, Vol. 10, No. 2 (Sl. No. 20), pp. 1804-1809
Geotech., Const. Mat. and Env., ISSN: 2186-2982(P), 2186-2990(O), Japan

DEVELOPMENT OF A PROBABILISTIC LIQUEFACTION POTENTIAL MAP FOR METRO MANILA

Dungca, Jonathan R.[1] and Chua, Renz Anderson D.[2]

[1]Civil Engineering Department, De La Salle University Manila, Philippines;

ABSTRACT: The study aimed to create a probabilistic liquefaction potential map for Metro Manila to help prepare for future calamities. A liquefaction opportunity map was produced by computing the probability of an earthquake with a moment magnitude of at least 5.2 from occurring. Historical data were gathered from 7 surrounding active faults within a 150 km radius of Metro Manila to determine their recurrence. A liquefaction susceptibility map was also developed by taking into consideration the conditions of the soil. Approximately 1000+ borehole logs scattered across Metro Manila was used in developing this map. These two maps were then combined to create the probabilistic liquefaction potential map. The results show that there is only a 2% chance of an earthquake capable of triggering a liquefaction occurring in a given year but in 50 years, there is a 10% chance of exceedance coming from an earthquake with an acceleration of 0.7g. The earthquake is most likely to come from the Valley Fault System which runs straight through Metro Manila.

Keywords: PSHA, Liquefaction Potential, Liquefaction Opportunity, Liquefaction Susceptibility

1. INTRODUCTION

Geotechnical hazards by definition are events that are directly caused by the action of the ground that would cause adverse effects on humanity. This includes but is not limited to earthquakes, liquefaction, soil settlement, soil heaving, collapse, land-slide and scouring [1].

The two geotechnical hazards, earthquake and liquefaction must continuously be looked out for. Since Manila is the capital of the Philippines, its vulnerability is that much greater than any other location in the country. In addition to that, the Metro also contains a lot of non-engineered houses which are in great risk as mentioned in [2]. This is why a study on the different geotechnical hazards must be done to prepare not just the professionals for their design but also for the normal individuals to protect their lives.

2. METHODOLOGY

2.1 Data Gathering

Determination of Source – In order to determine the active faults situated around the area of interest, the researcher first consulted the National Structural Code of the Philippines (NSCP) to see which among the known faults are within the 150km radius of NCR. This 150km radius is in accordance to [3].

Earthquake Records – Records of earthquakes from the faults determined above having values not less than 5.2 in magnitude in the Richter's scale were gathered as can be seen in Fig. 1.

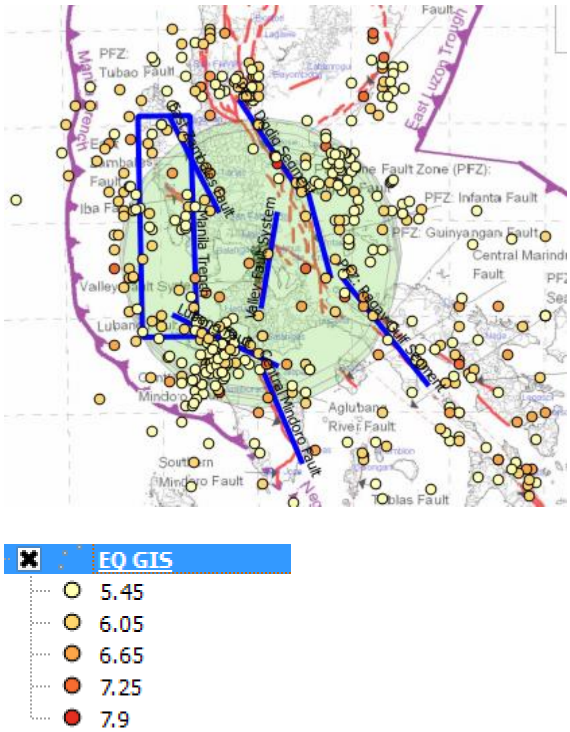

Fig. 1 Spread of EQ events in the area of study

Source Characteristics – This included its geometry, source type, and direction of movement that can affect the modelling of each earthquake generator.

Borehole Logs – These contain vital soil information that show the susceptibility of the soil at hand. These were then inputted into ArcGIS and used the spatial analysis tools, ordinary Krigging, one of the eight interpolation techniques mentioned in [4].

2.2 Data Analysis

Magnitude Limits – Magnitude 5.2 served as the lower limit in this study because according to [5] this surface magnitude was the smallest earthquake that was able to trigger liquefaction. This happened in Laoag city in the Northern parts of Luzon. The upper limit used was a magnitude of 8.2 since it is the largest earthquake ever recorded in the country [6]. It should be noted that both these limits are in terms of surface magnitude, the most common type of magnitude recorded in the country. It is to be expected that the data will not have a significant spread throughout all the magnitude between the said ranges above so to cover this problem, an interval of 0.6 magnitudes will be used as a range to ensure that each group will have enough data within it. This interval range was adopted from the work of [7] where he had found out that this range is the most effective way of distributing the data points without hindering the study's results.

Modelling of the Earthquake Events –First assumption is that surface magnitudes below or equal to 5.7 were considered to come from a point source since the magnitude is relatively small in comparison [8]. On the other hand, those that exceed this value were considered as either a linear fault rupture or an area rupture depending on the generator's geometry and source type. The second assumption was that both linear fault and area fault ruptures will follow the finite fault rupture model by [9] which states that the earthquake generated at the focus will propagate and felt equally along the rupture length or area. The relationship between length and the moment magnitude of a strike slip fault is expressed by Eq. (1) [10].

$$\log L = 0.74M_w - 3.55 \quad \sigma_{\log L} = 0.23 \tag{1}$$

Despite having the equation in terms of moment magnitude, the models Eq. (2) and Eq. (3) developed by [11] successfully converted the surface and body wave magnitude available in the country into moment magnitude so that it can be used in this equation.

$$M_w = e^{-0.222+0.233M_s} + 2.863 \tag{2}$$
$$M_w = e^{-4.664+0.859M_b} + 4.555 \tag{3}$$

Equation (4) on the other hand uses a model that was derived from a database containing earthquakes from subduction zones. This equation was then used to determine the area fault rupture of the event by applying the determined length value in the aspect ratio prepared by [12].

$$M = 4.532 + 0.887\log L \qquad \sigma_M = 0.344 \tag{4}$$

where:
$L = 2W$

Probability Distribution of distance R – To determine P(R), the assumption made was that the radius used in solving for the probability is the nearest distance between the point of interest and a splice or part of the rupture area or length. This was made in accordance to the finite fault rupture model by [9] where it states that an earthquake has an equal probability of occurrence in the whole length or area of the fault rupture area or length. For an area source type, the region of permissible foci needs to be determined first. This region was then divided into 1 square kilometer, placing the focus on the center of each grid. This origin was then extended in accordance to the aspect ratio of the magnitude interval used. The shortest distance from that area to the site will be taken as R. To compute for the probability distribution of R, the number of ruptures that falls on each 10 km distance interval must be normalized by the total number of ruptures possible for the source zone. The same concept was used for linear source types except that instead of dividing into 1 square km intervals, the length of rupture was divided into 1km interval. The length was then extended from the origin of each interval. This will give the value R. The computation for P(R) was the same as above [8].

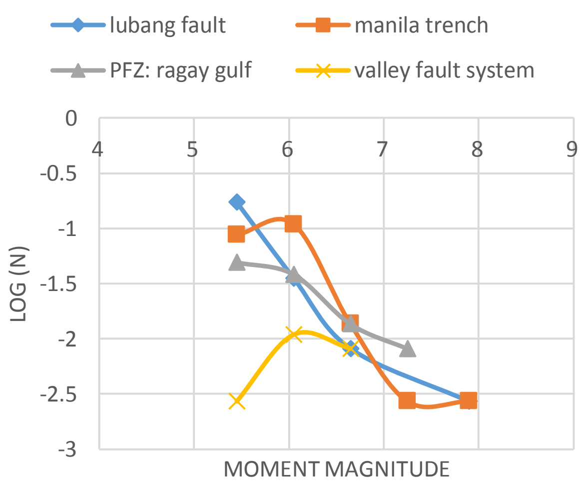

Fig. 2 Annual rate of occurrence

Annual Rates of Earthquake Activity – The annual rate of activity in Fig. 2 for each seismic generator was made by distributing each recorded earthquake event to the source nearest to its epicenter. The number of events per magnitude range per generator divided by the total number of years that has available record resulted to the annual rates of earthquake activity. This was repeated every magnitude range to every available faults. A Semi-logarithmic regression was also made from the values determined and was used for determining the next variable needed.

Probability Distribution of Earthquake Magnitude M – This can be done by using Eq. (6) by [13]. The $\boldsymbol{\beta}$ used in the equation was the absolute value of the slope determined from the regression mentioned above. Multiplying the results to the probability values of R for each interval for each source and then combining all of them will result to the probability of occurrence of earthquakes that can cause liquefaction to occur at a specific location.

$$f_M(m) = \frac{\beta \exp[-\beta(m-m_l)]}{1-\exp[-\beta(m_u-m_l)]} \tag{5}$$

$$P[m_l \leq m \leq m_u] = \int_{m_l}^{m_u} f_M(m) \approx f_M\left(m_l + \frac{m_u}{2}\right)(m_u - m_l) \tag{6}$$

Ground Motion Intensity – Because of the lack of strong ground motion data in the country, the attenuation relationship, Eq. 7, developed by [14] with a similar tectonic setting was used instead.

$$\log A = 0.41M - \log(R + 0.032 \times 10^{0.41M}) - 0.0034R + 130$$
$$\sigma_{\log A} = 0.21 \tag{7}$$

Given the value of A, the probability that a target PHA (a*) was then exceeded should an earthquake of the given magnitude interval occur at the given distance range, P(A), can be estimated by computing the standard normal deviation z Eq. (8) and then obtaining the cumulative distribution function (CDF) value [8].

$$z* = \frac{\log a* - \log A}{\sigma_{\log A}} \tag{8}$$

Correction Factors on N value – The N value shown in the borehole logs cannot be used directly in the succeeding equations needed in determining the liquefaction susceptibility. The N value needed to be adjusted first by several correction factors before it can be used. This was done by using Eq. (9) and Eq. (10) by [15]. The summary of the results can be seen in Fig. 3.

$$N_{60} = NC_N C_E C_B C_R C_S \tag{9}$$

where:
N_{60} - corrected N value;
N - standard N value;
C_N - factor to normalize N to a common reference effective over burden stress;
C_E - correction for hammer energy ratio;
C_B - correction for borehole diameter;
C_R - correction for rod length;
C_S - correction for samplers;

$$N_{60cs} = \alpha + \beta N_{60} \tag{10}$$

where:
$\alpha = 0 \; for \; FC \leq 5\%$
$\alpha = e^{1.76-\left(\frac{190}{FC^2}\right)} \; for \; 5\% < FC < 35\%$
$\alpha = 5 \; for \; FC \geq 35\%$
$\beta = 1 \; for \; FC \leq 5\%$
$\beta = 0.99 + \frac{FC^{1.5}}{1000} \; for \; 5\% < FC < 35\%$
$\beta = 1.2 \; for \; FC \geq 35\%$

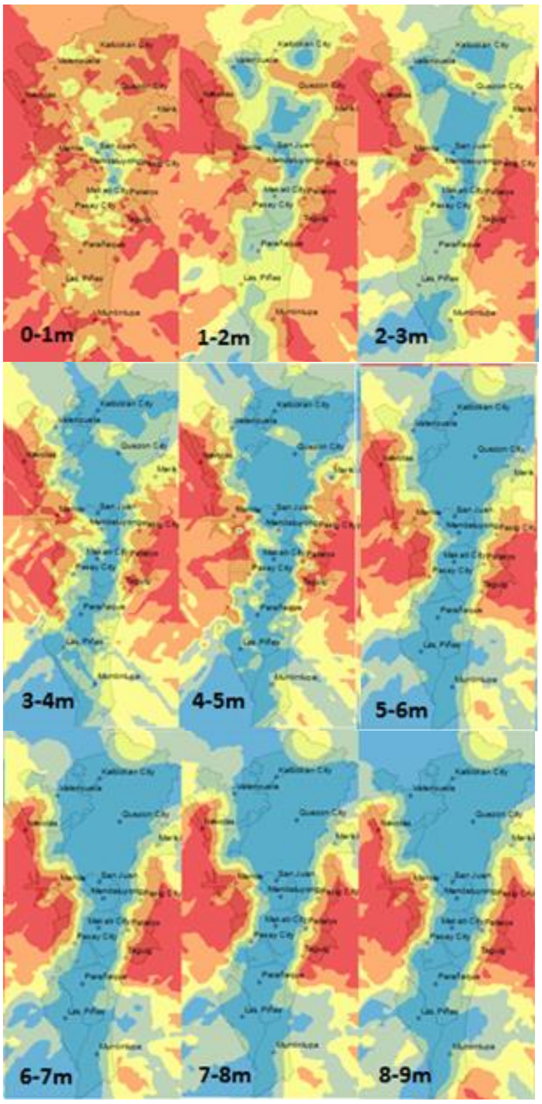

Fig. 3 SPT value per meter depth

$\boldsymbol{CRR_{7.5}}$ – With the corrected value of $\boldsymbol{N_{60cs}}$, $\boldsymbol{CRR_{7.5}}$ was then determined by Eq. (11) developed by [15]. Equation (12) and Eq. (13) were then used to adjust this value to the right magnitude and overburden pressure.

$$CRR_{7.5} = \frac{1}{34-N_{60}} + \frac{N_{60}}{135} + \frac{50}{(10N_{60}+45)^2} - \frac{1}{200} \tag{11}$$

$$K_M = \frac{10^{2.24}}{M_w^{2.56}} \qquad (12)$$

$$K_\sigma = \left(\frac{\sigma'_v}{P_a}\right)^{f-1} \qquad (13)$$

CSR and the 'a' to trigger – From the value determined above, given a factor of safety of 1.3, the value for CSR was determined. This value was then equated to Eq. (14) developed by [16] to determine the acceleration needed to possibly trigger a liquefaction. This acceleration can then be used to determine the susceptibility of the area and subsequently its liquefaction potential also.

$$CSR = \frac{0.65 a_{max} \sigma_{vo} r_d}{g \sigma'_{vo}} \qquad (14)$$

where:

a_{max} - peak horizontal acceleration

$r_d = 1 - 0.00765z \; for \; z \leq 9.15m$

$r_d = 1.174 - 0.0267z \; for \; 9.15m < z \leq 23m$

Results

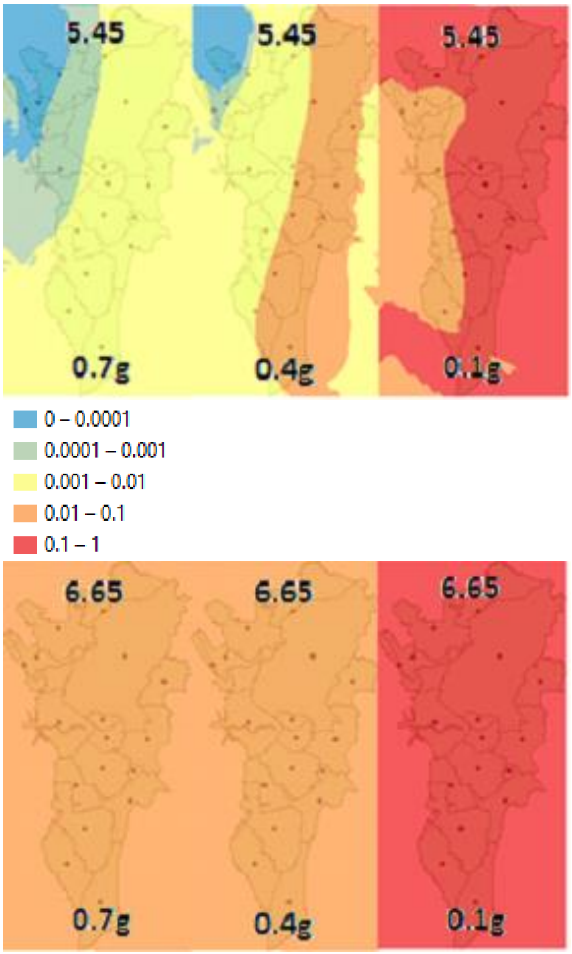

Fig. 4 Liquefaction Opportunity

Liquefaction Opportunity – Now that the values of P(R), P(A), P(M) and v_i are known for each magnitude interval. Substituting all these values into Eq. (15) resulted to the annual exceedance rate for various target PHAs in each source.

$$\lambda[X \geq x] \approx \sum_{sources\, i} v_i \int_{Mo}^{Mmax} \int_{R|M} P[X \geq x|M, R] f_m(m) \, f_{R|M}(r|m) dr dm \qquad (15)$$

Combining them together will produce the annual rate of exceeding a target PHA when an earthquake capable of triggering liquefaction occurred at any of the sources nearby as can be seen in Fig. 4.

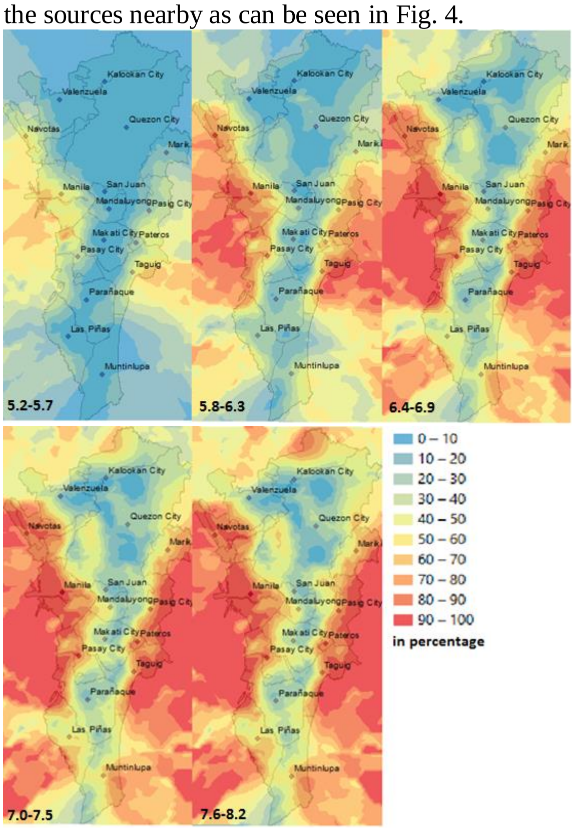

Fig. 5 Liquefaction Susceptibility

Liquefaction Susceptibility – Given that an earthquake with a specific magnitude range from a fixed distance of 15km to the target site, the probability of exceeding the target acceleration that is needed to trigger the event by the acceleration by the given magnitude range and fixed distance was then computed. Example of results can be seen in Fig. 5.

Liquefaction Potential – Assimilating both the liquefaction opportunity and susceptibility produced a liquefaction potential map for the site. Figure 7 showed the probability of exceeding the acceleration needed to trigger a liquefaction by combining every combination of magnitude and distance for every seismic generator around the area.

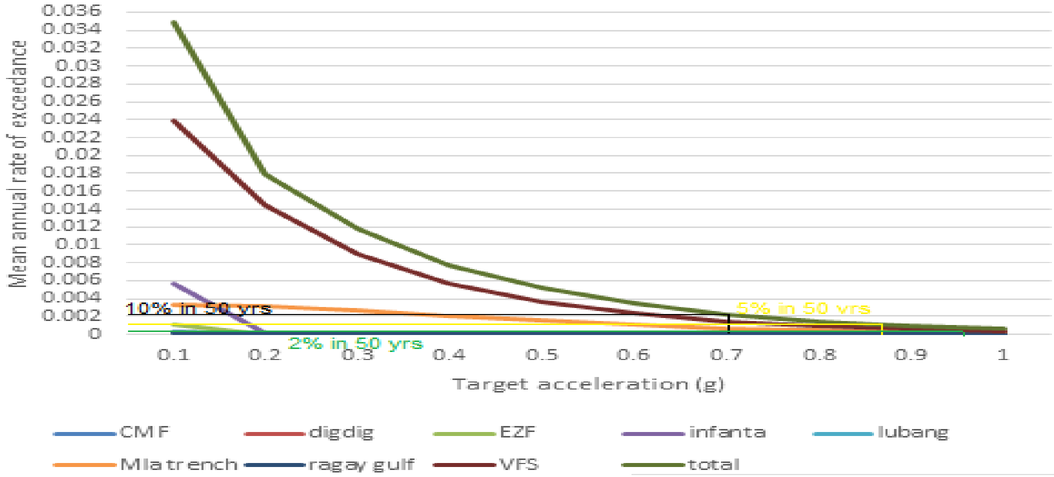

Fig. 6 Hazard Curve for all seismic generators

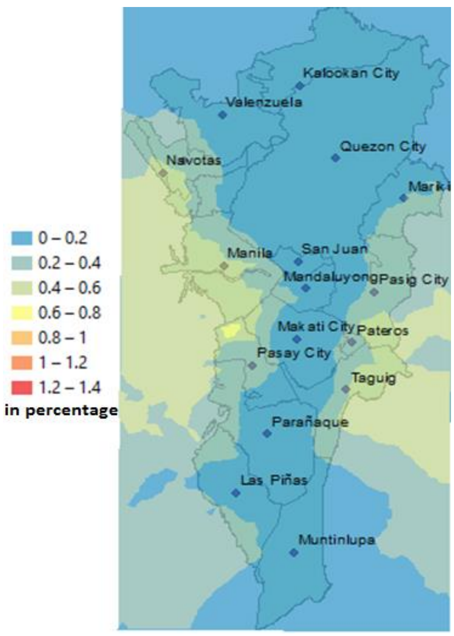

Fig. 7 Liquefaction Potential for Metro Manila

Design Ground Motion – Aside from the annual probability that the target acceleration (a*) will be exceeded should an earthquake capable of triggering liquefaction occurred in any of the source zones, $\lambda[X \geq x]$, it is also necessary to compute the PHA corresponding to a given probability of exceedance in a given time frame. The design ground motion used in this study was a 10% probability of exceedance in a 50 year time frame Eq. (16) [8].

$$\lambda_{y*} = \frac{\ln(1-P[Y_T > y*])}{T} = \frac{\ln(1-0.1)}{50} = 0.00211 \qquad (16)$$

Hazard Curve – The resulting values was then used to generate hazard curves for the liquefaction opportunity as can be seen in Fig. 6.

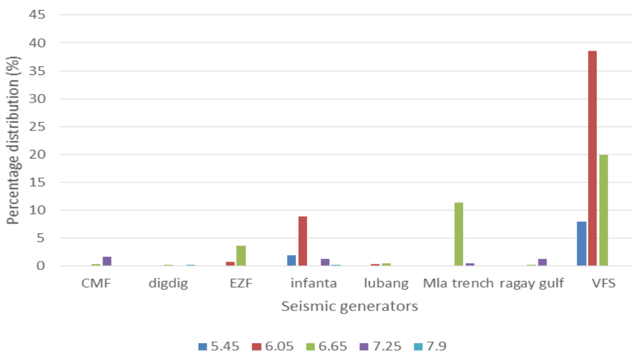

Fig. 8 Deaggregation of results

Deaggregation – The results was then be deaggregated, as shown in Fig. 8, to show which among the magnitude intervals will be responsible in the occurrence of the most probable earthquake that will cause liquefaction in the area of interest. It also showed which among the seismic generators contribute the most to the probabilities. This knowledge can then be used to make to prepare for the worst and properly mitigate and lessen the damages that will be incurred by the phenomenon.

3. CONCLUSION

From the earthquake opportunity analysis, the greatest probability of an earthquake with a magnitude of at least 5.2 has only 1% chance of occurring within a given year but if we look at the seismic hazard map, one could see that in the next 50 years, there is a 10% chance of having an earthquake generate an acceleration of 0.7g in the area which is a bit higher to the 0.6g value determined by [7]. This value, according to the deaggregation, would likely come from the valley fault system with a magnitude range of 5.8 – 6.3 from a distance range of 0 – 10km away from the site.

The vertical mid-section of the Metro Manila has very hard soil in it though they start showing at around 3m deep. Both the western and eastern part of the region has sandy top soil for the first 6 meters, beyond that it is mostly clays and silts. On the other hand, SPT values show a much more constant range of values throughout the entire 20m depth. Seeing that the top soil for all seem to be red and yellow in color even for the vertical mid-section of the region. This is because this layer of soil have not been consolidated yet. After that the red and yellow section continue to cluster in the same area where the sandy soils are found, both in the western and eastern part of the region. Since the liquefaction susceptibility of the area is largely influenced by the soil type map and SPT map, it was no surprise that the patterns shown in the susceptibility maps are pretty much the same in nature.

Next, the liquefaction potential developed from this study shows the same pattern as that of the susceptibility except the values are very much lower, the greatest probability only having a 2% chance of exceedance in a given year. But just like with the earthquake opportunity map, this should not be underestimated since this value increases as time passes by.

These results can now be used to help prepare the government of upcoming threats caused by earthquakes and liquefactions. Countermeasures can now be implemented to minimize if not completely take away the destructive effects of these events. One possible countermeasure would be to use crushed tiles as backfill to reduce the effects of liquefaction [17]. With the present maps, one could also design structures that could withstand an acceleration of 0.7g.

4. REFERENCES

[1] Orense R P, Geotechnical Hazard: Nature, Assessment and Mitigation, Quezon City: The University of the Philippines Press, 2003.

[2] Putra R R, Kiyono J, Furukawa A, “Vulnerability assessment of non engineered houses based on damaged data of the 2009 Padang earthquake in Padang City, Indonesia” International Journal of GEOMATE Vol 7 (2), 2014, pp. 1076-1083.

[3] Yould T, Perkins D, “Mapping liquefaction induces ground failure potential” Journal of the Geotechnical Engineering Division, ASCE 104 (4), 1978, pp. 443-446.

[4] Al-Ani H, Eslami-Andargoli L, Oh E, Chai G, “Categorising geotechnical properties of surfers paradise soil using geographic information system (GIS)” International Journal of GEOMATE Vol 5 (2), 2013, pp. 690-695.

[5] SEASEE (Southeast Asia Association of Seismology and Earthquake Engineering), Series on Seismology vol IV, 1985.

[6] Phivolcs (Philippines Institute of Volcanology and Seismology), Catalogue of Mentro Manila Earthquakes, magnitude 5.2 and above (1907 – 2013), 2014.

[7] Thenhaus P, Hanson S, Algermissen S, Bautista B, Bautista M B J P, et al., “Estimates of the regional ground motion hazard in the Philipiines. National Disaster Mitigation in the Philipines.” DOST-PHIVOLCS, 1994, pp. 45-60.

[8] Beroya M & Aydin A, “Seismic hazard analysis of Laoag City, Northern Philippines for liquefaction potential assessment”, Engineering Geology 96, 2008, pp. 28-42.

[9] Kiureghian D & Ang A, “A fault rupture model for seismic risk analysis”, Bulletin of the Seismological Society of America 67, 1977, pp. 1173-1194.

[10] Wells D, Coppersmith K, “New empirical relationships among magnitude, rupture length, rupture width, rupture area and surface displacement” Bulletin of the Seismological Society of America 84 (4), 1994, pp. 974-1002.

[11] Giacomo D, Bondar I, Storchak D A, Engdhal E R, Bormann P, Harris J, “ISC-BEM: Global Instrumental Earthquake Catalogue (1900-2009), III. Re-computed Ms and mb, proxy Mw, final magnitude composition an completeness assessment”, Physics of the Earth and Planetary Interiors, 2014.

[12] Geller R, “Scaling relations for earthquake source parameters and magnitudes”, Bulletin of the Seismological Society of America 80 (5), 1976, pp. 757-776.

[13] Kramer S, Geotechnical Earthquake Engineering, New Jersey: Prentice Hall, 1996.

[14] Fukushima Y & Tanaka T, “A new attenuation relationship for peak horizontal acceleration of strong earthquake ground motion in Japan”, Bulletin of the Seismological Society of America 80, 1990, pp. 1501-1523.

[15] Youd T, Idriss I, Andrus R, Seed, “Liquefaction resistance of soils summary report from 1996 NCEER and 1998 NCEER/NSF workshops on Evaluation of Liquefaction Resistance of Soil” Journal of Geotechnical and Geoenvironmental Engineering, ASCE 127. 2001, pp. 817-833.

[16] Seed H B, Idriss I M, “Simplified procedure for evaluating soil liquefaction potential”, J. Geotech Engrg. Div., 1971, pp. 1249-1273.

[17] Morikawa Y, Maeda K, Zhang F, “Effectiveness of crashed tile in countermeasure against liquefaction”, International Journal of GEOMATE Vol 7 (1), 2014, pp. 1003-1008.

Int. J. of GEOMATE, April, 2016, Vol. 10, No. 2 (Sl. No. 20), pp. 1804-1809.

MS No. 5191j received on June 15, 2015 and reviewed under GEOMATE publication policies.

Corresponding Author: Dungca, Jonathan R.